

Visualization of Hepatic Uptake Transporter Function in Healthy Subjects by Using Gadoteric Acid–enhanced MR Imaging¹

Ali Nassif
Jia Jia
Markus Keiser, MD
Stefan Oswald, PhD
Christiane Modess, MD
Stefan Nagel, PhD
Werner Weitschies, PhD
Norbert Hosten, MD
Werner Siegmund, MD
Jens-Peter Kühn, MD

Purpose:

To determine if genetic polymorphisms of liver-specific human organic anion transporting polypeptide (OATP) 1B1 and OATP1B3 influence cellular uptake of gadoteric acid in vitro and if functionally relevant polymorphisms are confounders for liver enhancement by gadoteric acid in healthy subjects.

Materials and Methods:

This study received ethics approval, and all subjects provided written informed consent. Cellular uptake of gadoteric acid by OATP1B1 and OATP1B3 and their frequent genetic variants was measured by using stable transfected embryonic kidney HEK293 cells. Liver signal intensity at gadoteric acid–enhanced MR imaging and pharmacokinetics of gadoteric acid were evaluated in 36 healthy carriers of *SLCO1B1/1B3* wild-type alleles ($n = 10$), *SLCO1B1**1b/*1b ($n = 8$), *SLCO1B1**15/*15 ($n = 7$), *SLCO1B1**5/*15 ($n = 1$), *SLCO1B1**1a/*5 ($n = 6$), and *SLCO1B3**4/*4 ($n = 4$) by using T1-weighted MR imaging and liquid chromatography tandem mass spectrometry.

Results:

Transport activity for gadoteric acid was increased in cells transfected with *SLCO1B1*c.388A>G (12.8 pmol/[mg·min] ± 3.53, $P = .001$) but decreased in cells with *SLCO1B1*c.388A>G/521T>C (3.11 pmol/[mg·min] ± 0.918, $P = .004$) compared with cells with nonvariant transporter (6.32 pmol/[mg·min] ± 2.73). Compared with activity of cells transfected with the nonvariant *SLCO1B3* (7.43 pmol/[mg·min] ± 2.43), *SLCO1B3*c.699G>A was a gain-of-function variant (15.1 pmol/[mg·min] ± 5.52, $P = .002$), whereas *SLCO1B3*c.334T>G (0.364 pmol/[mg·min] ± 0.125, $P = .0001$) and *SLCO1B3*c.1564G>T (0.295 pmol/[mg·min] ± 0.247, $P = .0001$) were variants with lower function. Liver enhancement with gadoteric acid was reduced in subjects with OATP1B1*1a/*5 compared with wild-type subjects and those with OATP1B1*1b/*1b (area under enhancement curve, 3–480 minutes in arbitrary units [au]; 20.7 au ± 6.85 vs 36.5 au ± 8.08 [$P = .006$] vs 34.6 au ± 8.92 [$P = .026$]). The OATP1B3*4 polymorphism was not of functional relevance. No pharmacokinetic characteristics of gadoteric acid were influenced by genetic polymorphisms of OATP1B1 and OATP1B3.

Conclusion:

Liver-specific OATP1B1 and OATP1B3 are uptake carriers for gadoteric acid in subjects. Genetic polymorphisms of OATP1B1 are signal confounders in gadoteric acid–enhanced liver MR imaging.

©RSNA, 2012

Supplemental material: <http://radiology.rsna.org/lookup/suppl/doi:10.1148/radiol.12112061/-/DC1>

¹From the Department of Clinical Pharmacology (A.N., J.J., M.K., S.O., C.M., W.S.), Department of Biopharmacy and Pharmaceutical Technology (S.N., W.W.), and Department of Radiology and Neuroradiology (N.H., J.P.K.), Ernst-Moritz-Arndt University Greifswald, Ferdinand-Sauerbruch-Strasse NK, Greifswald D-17475, Germany. Received September 27, 2011; revision requested December 6; revision received January 14, 2012; accepted February 15; final version accepted March 19. Supported by grants O3IP612 (InnoProfile) and O3IS2061A (Greifswald Approach to Individualized Medicine) from the German Federal Ministry for Education and Research. Address correspondence to J.P.K. (e-mail: kuehn@uni-greifswald.de).

Contrast material-enhanced magnetic resonance (MR) imaging with liver cell-specific gadoxetic acid enables improved detection of hepatic lesions when compared with other extracellular nonspecific MR imaging contrast agents, and it is superior in the diagnosis and therapeutic management of focal liver lesions when compared with computed tomography (1–4). Areas without hepatocytes (eg, metastases, cysts, or abscesses) lack positive enhancement (5,6). On the other hand, positive enhancement may occur in focal lesions of hepatocellular origin. Some hepatocellular carcinomas show even paradoxical hyperintense enhancement, depending on the degree of differentiation (7–11). It is important to note from clinical practice that enhancement of the liver parenchyma is highly variable, and it is readily understood that insufficient enhancement in some patients may be related to liver dysfunction (12–15). An understanding of the specific uptake mechanism or mechanisms for gadoxetic acid from the sinusoidal blood into the liver is a precondition to predict signal intensity in patients and to identify the confounders for variability of signals.

There is evidence from transport studies in which researchers used *Xenopus laevis* oocytes and drug interaction studies in rats that candidates for hepatic uptake of gadoxetic acid in human subjects are members of the organic anion-transporting polypeptides (OATP) family and bile salt transporters (16–19). Our

group has shown by using stable transfected embryonic kidney (HEK) cells that gadoxetic acid is a substrate of the human Na⁺/taurocholate cotransporting polypeptide and the liver-specific human OATP1B1 and OATP1B3 but not of the ubiquitous human OATP2B1 (20). However, so far it is unclear to what extent the liver-specific uptake transporters affect the hepatic enhancement with gadoxetic acid at clinical MR imaging. One approach to prove the clinical relevance of OATP1B1 and OATP1B3 for the diagnostic use of gadoxetic acid is to evaluate its pharmacokinetics and liver enhancement in selected healthy subjects with functionally relevant genetic polymorphism of the candidate transporters. OATP1B1 and OATP1B3 must be considered major variables in the clinical use of gadoxetic acid if there are substantial differences in pharmacokinetics and liver enhancement in subjects belonging to the group of normal transporters (subjects carrying wild-type alleles), poor transporters (subjects carrying loss-of-function variants), or extensive transporters (subjects carrying gain-of-function variants) (21–23). Thus, the objectives of our study were to determine whether genetic polymorphisms of

OATP1B1 and OATP1B3 influence cellular uptake of gadoxetic acid in vitro and to determine whether functionally relevant polymorphisms are confounders for liver enhancement by gadoxetic acid in healthy subjects.

Materials and Methods

Appendix E1 (online) describes the role of liver-specific uptake transporters, biliary secretion of gadoxetic acid, and gene structure for OATPs.

In Vitro Study with Human OATP1B1 and OATP1B3

Cell culture, cloning and transfection.—HEK cells stably transfected with human OATP1B1 and OATP1B3 were generated and cultured as described previously (20). The following genetic polymorphisms were generated with site-directed mutagenesis, as follows: (a) *SLCO1B1*c.388A>G (p.Asn130Asp, rs2306283), *SLCO1B1*c.521T>C (p.Val174Ala, rs4149056), and *SLCO1B1*c.388A>G/521T>C (p.Asn130Asp/Val174Ala) and (b) *SLCO1B3*c.334T>G (p.Ser112Ala, rs4149117), *SLCO1B3*c.699G>A (p.Met233Ile, rs7311358), *SLCO1B3*c.1564G>T (p.Gly522Cys, rs72559743), and *SLCO1B3*c.334T>G/699G>A (p.Ser112Ala/Met233Ile).

Implications for Patient Care

- Dynamic gadoxetic acid-enhanced liver MR imaging has the potential to quantify the hepatic multidrug transporter function.
- Reduced hepatic uptake of gadoxetic acid caused by genetic polymorphism of OATP1B1 could affect the visualization of focal lesions in some patients.
- Administration of gadoxetic acid should be avoided for 2–3 hours after oral administration of cholesterol-lowering drugs (atorvastatin), immunosuppressants (cyclosporine, tacrolimus), and human immunodeficiency virus protease inhibitors (nelfinavir, ritonavir, saquinavir), and glibenclamide, paclitaxel and rifampicin.

Advances in Knowledge

- The activity of the liver-specific human drug transporter organic anion-transporting polypeptide (OATP) 1B1 may be used to predict the signal intensity in gadoxetic acid-enhanced liver MR imaging.
- Liver enhancement by gadoxetic acid in healthy subjects can be reduced by approximately 30%–40% by genetic polymorphisms of the hepatic uptake transporter OATP1B1.

Published online before print

10.1148/radiol.12112061 Content code: GI

Radiology 2012; 264:741–750

Abbreviations:

AUC = area under the receiver operating characteristics curve

BSP = bromosulphthalein

HEK = transfected embryonic kidney

OATB = organic anion-transporting polypeptide

Author contributions:

Guarantors of integrity of entire study, W.S., J.P.K.; study concepts/study design or data acquisition or data analysis/interpretation, all authors; manuscript drafting or manuscript revision for important intellectual content, all authors; approval of final version of submitted manuscript, all authors; literature research, A.N., J.J., M.K., S.O., W.W., W.S., J.P.K.; clinical studies, A.N., M.K., S.O., C.M., W.W., W.S., J.P.K.; statistical analysis, M.K., S.O., S.N., J.P.K.; and manuscript editing, A.N., M.K., S.O., W.W., N.H., W.S., J.P.K.

Potential conflicts of interest are listed at the end of this article.

See also the editorial by Sahani et al in this issue.

The variant alleles were introduced into vectors pQCXIN-OATP1B1 and pQCXIN-OATP1B3, respectively, by using the QuickChange site-directed mutagenesis kit (Stratagene, Amsterdam, the Netherlands) according to manufacturer instructions. The primers to generate the plasmids pQCXIN-OATP1B1*1b and pQCXIN-OATP1B1*5 were 5'-GTATTCCTAAAGAACTAATATC-GATTCATCAGAAAATTCAACATC-3' and 5'-GAATCTGGATCCTACATGTG-GATATATGCGTTCATGGGTAATATG-3', respectively. Plasmids pQCXIN-OATP1B3699G>A, pQCXIN-OATP1B3699G>A, and pQCXIN-OATP1B3 1564G>T were generated with 5'-GGAATCGGATCCATTTTGACATCTTTACCA-CATTTCTTCATG-3', 5'-GGATCTCTGTTTGCTAAAATGTACGTGGACATTG-GATATCTAG-3', and 5'-CAGAAAT-TACTCAGCGCACTTGTGTGAATGCCCGCCGGATAATAC-3', respectively. Accuracy of the mutagenesis was confirmed with sequencing. After infection of HEK293 cells, the clones were characterized with Western blot analysis and immunofluorescence staining, as described previously (20). The amount of transporter proteins localized to the cell surface was assessed with the biotinylation method by using the Cell Surface Protein Isolation Kit (Pierce, Rockford, Ill) according to the manufacturer instructions. After electrophoresis and Western blot analysis, the relative transport protein content was quantified by using Quantity One software (Bio-Rad, Munich, Germany).

In vitro assays.—All in vitro experiments were performed three times in triplicate by using 24-well plates (Greiner Bio-One, Frickenhausen, Germany), as described previously (20). In brief, 300 000 cells per well were seeded and cultivated in full growth medium for 2 days at 37°C by using a standard incubation buffer (24). In competition assays, OATP activity was measured with hydrogen 3 (³H) bromosulphophthalein (BSP) (14 Ci/mmol) (Hartmann Analytic, Braunschweig, Germany) as the substrate. ³H BSP was dissolved with unlabeled BSP (Sigma-Aldrich, Taufkirchen, Germany) to reach a final concentration of 0.05 μmol/L and 1 μmol/L for

OATP1B1 and OATP1B3, respectively. For quality control of all transfected cells, competition 100 μmol/L rifampicin (Riedel-DeHaën, Seelze, Germany)—a standard inhibitor for OATPs—was tested. After incubation for 5 minutes, cells were washed with ice-cold phosphate-buffered saline and lysed with 0.5% Triton-X-100 (Sigma, St Louis, Mo) and 0.5% sodium deoxycholate. Aliquots were mixed with 2 mL of a scintillation cocktail (Rotiszint Eco Plus; Roth, Karlsruhe, Germany). The ³H BSP content was measured by using a scintillation beta counter (LKB-Wallac, Turku, Finland). The uptake of gadoxetic acid (0.016, 0.03, 0.06, 0.125, 0.25, 0.5, and 1.0 mmol/L) by OATP1B1 and OATP1B3 and their genetic variants was quantified after incubation for 10 minutes with liquid chromatography tandem mass spectrometry (20).

MR Imaging and Pharmacokinetic Study Protocol

Subjects.—The study protocol was approved by the German Federal Department of Drugs and Medicinal Products and by the independent Ethics Committee of the University Medicine of Greifswald and was registered by EudraCT (2006-005249-13) and www.ClinicalTrials.gov (NCT01420211). All subjects provided written informed consent before they were included in this pharmacogenomic study. The study included 36 healthy subjects (mean age, 27 years; range, 21–44 years) with a mean body mass index of 23.7 kg/m² (range, 19.2–28.5 kg/m²). A total of 16 subjects were women (mean age, 27 years; range, 22–44 years) with a mean body mass index of 22.4 kg/m² (range, 19.2–26.4 kg/m²), and 20 subjects were men (mean age, 27 years; range, 21–36 years) with a mean body mass index of 24.7 kg/m² (range, 21.9–28.5 kg/m²). The study population was recruited from our clientele of about 2000 genotyped healthy subjects. We included all available subjects in our study with the desired variant haplotypes (mentioned later in this article) who were available and who gave written informed consent. The sample size of groups with the following haplotypes or genotypes was as follows:

*SLCO1B1**1a/*1a, 10 subjects (wild-type protein); *SLCO1B1**1b/*1b, eight subjects; *SLCO1B1**15/*15, seven subjects; *SLCO1B1**5/*15, one subject; *SLCO1B1**1a/*5, six subjects; and *SLCO1B3**4/*4, four subjects. Because of the nearly complete linkage disequilibrium, the subjects with *SLCO1B3**4/*4 were most likely also carriers of *SLCO1B3**2/*2 (c.334TT, p.334Ser). All carriers of *SLCO1B1* variants were carriers of *SLCO1B3*c.334GG/699AA (p.112Ala/233Ile), which is the most frequent variant in healthy white subjects (23). Furthermore, all subjects included had wild-type *ABCC2* (protein name, multidrug resistance-related protein 2 [or MRP2]). Genotyping was performed with standard procedures, as described elsewhere (25,26).

We confirmed the subjects were in good health by taking each subject's history, performing a physical examination, and conducting routine clinical, chemical, and hematologic tests. The subjects were nonsmokers or smoked no more than 10 cigarettes per day and did not take any medication except hormonal contraceptives (women only). All subjects had negative results at screening for drugs, human immunodeficiency virus, hepatitis B virus, and hepatitis C virus. Intake of grapefruit-containing food or beverages and poppy seed-containing products was not allowed beginning 7 days prior to gadoxetic acid-enhancing imaging and lasting until the last sampling of feces (5 days after imaging). Drinking of alcohol was not permitted beginning 2 days before the study and lasting throughout the blood sampling period (48 hours).

Study procedures.—The subjects were admitted to the study unit in the evening before the pharmacogenomic study. After overnight fasting for at least 10 hours, they underwent dynamic contrast-enhanced MR imaging of the liver after intravenous administration of 0.025-mmol gadoxetic acid (0.1 mL per kilogram of body weight, Primovist/Eovist; Bayer Healthcare, Berlin, Germany) followed by 20 mL of saline with a power injector (Spectris Dual Head; Medrad, Volkach, Germany), both with a constant flow of 2 mL/sec. MR

imaging was performed with a 1.5-T system (Magnetom Symphony; Siemens Healthcare, Erlangen, Germany) by using a short T1-weighted gradient-echo sequence (Flash 3D; Siemens Healthcare) with fat saturation in the axial plane. The sequence was performed in 20 seconds with breath holding and the following image parameters: repetition time msec/echo time msec, 3.35/1.35; flip angle, 12°; matrix size, 374 × 512 pixels; section thickness, 3 mm; 64 sections, and no parallel imaging. The dynamic study consisted of an unenhanced data set followed by sets acquired 15, 60, and 90 seconds and 2, 3, 4, 5, 6, 7, 8, 9, 10, 20, 30, 40, 50, 60, 90, 120, 240, and 480 minutes after bolus injection of gadoxetic acid.

Venous blood from the contralateral forearm vein was collected before and 6, 11, 21, 31, 45, 65, 95, and 125 minutes and 3, 4, 6, 8, 12, 24, and 48 hours after injection. Urine was collected for 3 days after administration, and feces were collected for 5 days. Serum and aliquots of urine and feces were stored at a temperature of at least -20°C until quantitative analysis was performed. The method was validated between 2.5 and 1000 ng/mL in cell homogenates, between 5 and 4000 ng/mL in serum, and between 25 and 4000 ng/mL in urine and fecal samples and was shown to be of adequate specificity, precision (1.7%–12.9% of mean values), and accuracy (-7.6% to 11.5% of the nominal values) for all matrices (20).

Biometric Evaluation

Transporter kinetics were evaluated by using Origin 5.0 (OriginLab, Northampton, Mass). Michaelis-Menten constant (K_m) and maximum transport velocity (V_{max}) were calculated by using the equation $y = V_{max} \cdot x / (K_m + x)$, where x is substrate concentration and y is transport velocity. The uptake characteristics were corrected for the nonspecific uptake into control cells and the percentage of biotinylation relative to the respective nonvariant protein.

Pharmacokinetic evaluation.—Area under the receiver operating characteristics curve (AUC) was assessed up to the last sampling time above the limit

of quantification (AUC_{0-t}) and was extrapolated to infinity by using the trapezoidal method ($AUC_{0-\infty}$). Elimination half-life ($t_{1/2}$) and the fictive serum concentrations at time zero (C_0) were estimated by using log-linear regression analysis. Renal clearance (CL_R) and intestinal clearance (CL_I) were derived from the cumulative amounts of gadoxetic acid excreted into urine and feces, respectively, over $AUC_{0-\infty}$. The pharmacokinetic evaluation was performed by using the statistical software package SAS 9.0 (SAS Institute, Cary, NC).

Evaluation of hepatic enhancement.—Hepatic enhancement of gadoxetic acid was quantified with voxel-based volumetric measurement of mean signal intensity (SI) throughout the liver tissue by using Voxar3D (Toshiba Medical Visualization Systems, Edinburgh, Scotland). All data were evaluated with volumetric analyses of the mean signal intensity to each time point (SI_t). To exclude enhancement as caused by extracellular distribution of gadoxetic acid, the value after 3 minutes (SI_3) was defined as blank, as recommended by Vogl et al (3). The relative signal intensity (SI_{rel}^{3-t}) was calculated as follows: $SI_{rel}^{3-t} = SI_t - SI_3$. The area under the signal intensity time curve (AUC_{3-t}) was calculated with the trapezoidal rule. The maximum relative signal intensity (C_{max}) and the time of maximum relative signal intensity (T_{max}) were taken directly from the signal intensity-time curve.

Statistical evaluation.—Sample differences were evaluated by using analysis of variance with post hoc repeated sample evaluation and the Student t test with Bonferroni adjustment. The level of significance was set at $P < .05$. All assessments were performed by using the SPSS 19 statistical program (IBM, Armonk, NY).

Results

HEK cells were successfully transfected with nonvariant *SLCO1B1* and *SLCO1B3* and polymorphic *SLCO1B1c.388A>G*, *SLCO1B1c.521T>C*, *SLCO1B1c.388A>G/521T>C*, *SLCO1B3c.334T>G*, *SLCO1B3c.699G>A*, *SLCO1B3c.1564G>T*, and *SLCO1B3c.334T>G/699G>A*,

as confirmed with the Western blot bands with the expected molecular masses of 84 kDa for OATP1B1 and 120 kDa for OATP1B3. All transporters were localized to the cell surface with immunofluorescence analysis of the HEK cells (Fig 1). The percentage of biotinylation (the relative amount of the polymorphic transport protein localized to the cell membrane relative to the respective nonvariant protein) was 74.1% for OATP1B1 p.130Asp, 83.8% for OATP1B1 p.174Ala, 152% for OATP1B1 p.130Asp/174Ala, 109% for OATP1B3 p.112Ala, 122% for OATP1B3 p.233Ile, 205% for OATP1B3 p.522Cys, and 80.1% for OATP1B3 p.112Ala/233Ile. All cell models showed transport of the probe substrate BSP and rifampicin was a strong inhibitor for uptake. The transport activity of OATP1B1 p.130Asp/174Ala for BSP was significantly lower compared with that of the nonvariant protein and OATP1B1 p.130Asp (Fig 2).

Gadoxetic acid had similar affinity for all OATP1B1 proteins, as indicated by nearly identical Michaelis-Menten constant values. The activity of OATP1B1 p.130Asp for gadoxetic acid uptake was significantly higher (gain of function) than that of nonvariant OATP1B1, while the activity of OATP1B1 p.130Asp/174Ala was significantly lower (loss of function). OATP1B3 p.233Ile was a gain-of-function carrier for gadoxetic acid, whereas OATP1B3 p.112Ala and OATP1B3 p.522Cys were significant loss-of-function transporters compared with the nonvariant protein. OATP1B3 p.112A/233Ile also was of lower activity numerically (Fig 3, Table 1).

Liver enhancement by gadoxetic acid in human subjects was reduced in healthy subjects with OATP1B1*1a/*5 when compared with that in wild-type subjects and those with OATP1B1*1b/*1b (area under the enhancement curve, 3–480 minutes in arbitrary units [au]; OATP1B1*1a/*5: mean, 20.7 au ± 6.85; wild type: mean, 36.5 au ± 8.08 [$P = .006$]; OATP1B1*1b/*1b: mean, 34.6 au ± 8.92 [$P = .026$]). The group that included all subjects with at least one *5

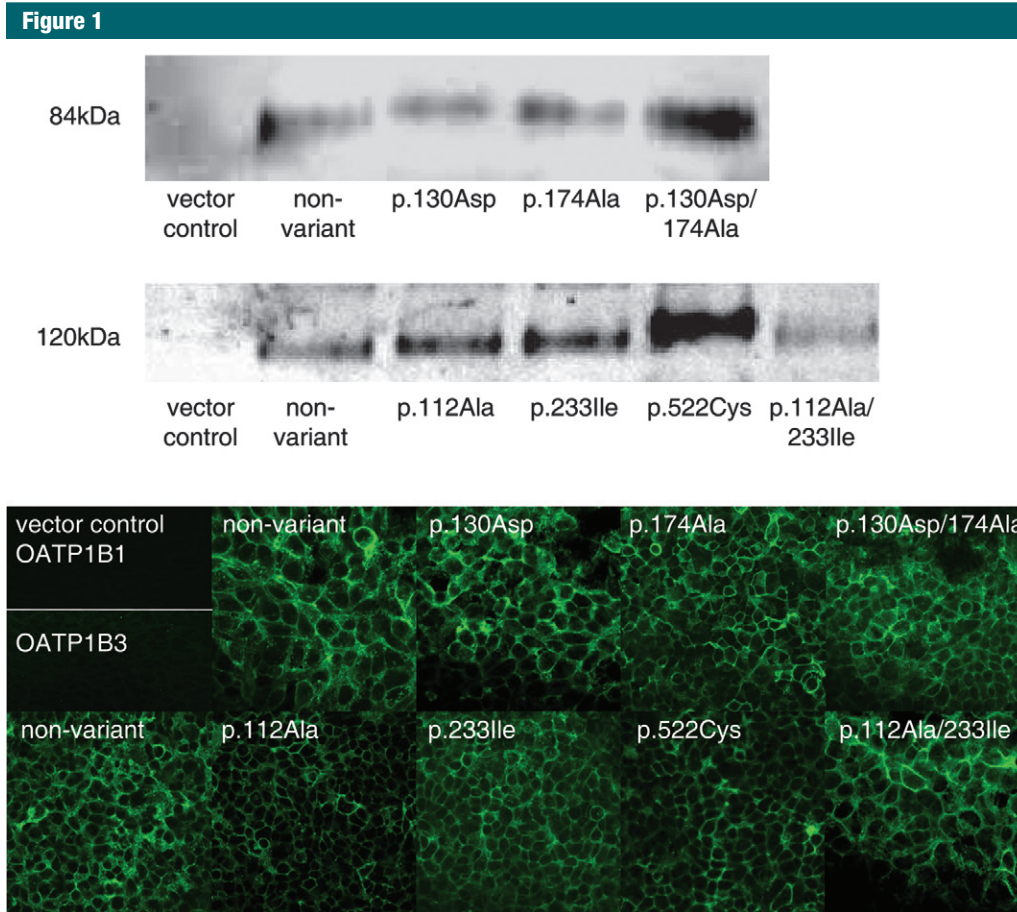


Figure 1: Western blot analysis (top and middle) and immunofluorescence staining of HEK cells (bottom) express nonvariant OATP1B1, OATP1B1 p.130Asp, OATP1B1 p.174Ala, and OATP1B1 p.130Asp/174Ala, as well as nonvariant OATP1B3, OATP1B3 p.112Ala, OATP1B3 p.233Ile, OATP1B3 p.522Cys, and OATP1B3 p.112Ala/233Ile.

allele (OATP1B1*1a/*5 and OATP1B1*15/*15) was also significantly different from the group with wild-type subjects (mean, 24.5 au \pm 8.39, $P = .005$). The OATP1B3*4 polymorphism was not functionally relevant for gadoxetic acid uptake in healthy subjects (Fig 4). None of the pharmacokinetic characteristics of gadoxetic acid, such as blood exposure, elimination half-life, or urinary and intestinal excretion were significantly influenced by the genetic polymorphisms of OATP1B1 and OATP1B3 (Table 2).

Discussion

Gadoxetic acid is a contrast agent used in MR imaging for which specific parenchymatous enhancement can only be

observed in the liver. Gadoxetic acid shares basic physicochemical properties of several OATP substrates, such as large molecule size (molecular weight, 725.72 Da) and anionic moiety. In our in vitro study, we confirmed our previous findings that gadoxetic acid is a substrate for the liver-specific human uptake transporters OATP1B1 and OATP1B3 (20). OATP1B1 and OATP1B3 represent members of the OATP superfamily that mediate the sodium-independent hepatic uptake of a diverse range of amphiphilic organic compounds along the basolateral (sinusoidal) membrane of hepatocytes, including bile acids, thyroid hormones, bilirubin glucuronides, steroid conjugates, and numerous drugs, such as statins or sartans. Thus, both OATPs exert a substantial role in disposition

and excretion of numerous drugs. Importantly, both carriers are susceptible to clinical drug-drug interactions—such as those caused by the strong inhibitors rifampin and cyclosporine or by several human immunodeficiency virus-protease inhibitors—and both carriers have clinically relevant genetic polymorphisms (21). In our in vitro study in which we used OATP-transfected HEK-cells, it became evident that frequently occurring single nucleotide polymorphisms of OATP1B1 and OATP1B3 are also of functional relevance for cellular uptake of gadoxetic acid. The *SCLO1B1*c.521T >C single nucleotide polymorphism leads to exchange of p.Val174Ala in the fourth transmembrane domain of the transport protein, which is consistently associated with reduced activity

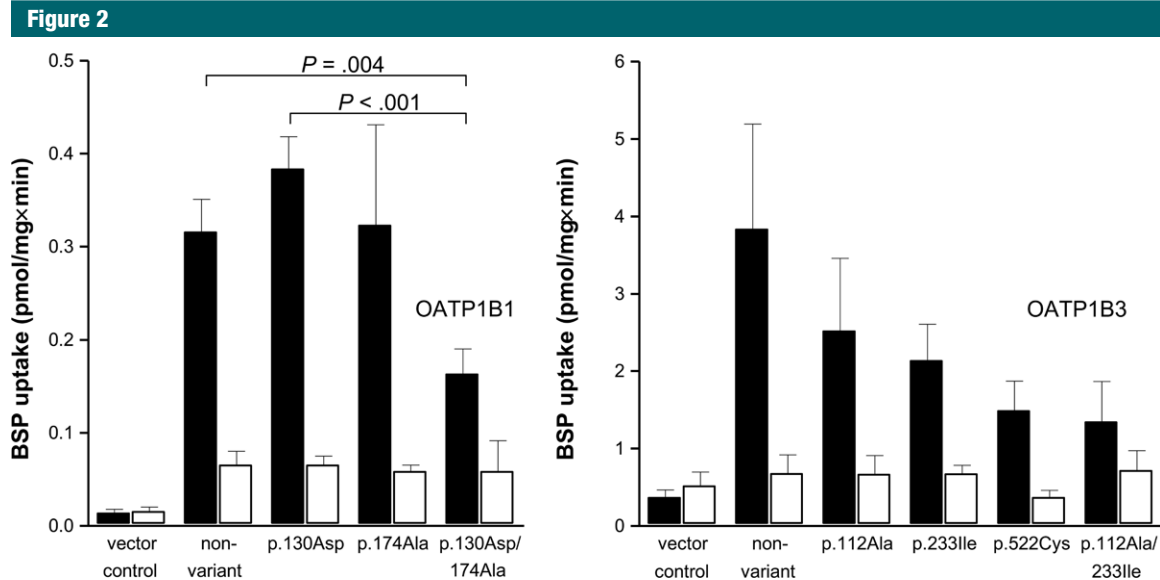


Figure 2: Bar graphs show uptake of BSP (black bars) in HEK cells expressing human nonvariant OATP1B1, OATP1B1 p.130Asp, OATP1B1 p.174Ala, and OATP1B1 p.130Asp/174Ala (left); nonvariant OATP1B3, OATP1B3 p.112Ala, OATP1B3 p.233Ile, OATP1B3 p.522Cys, and OATP1B3 p.112Ala/233Ile (right); and inhibition of BSP uptake by rifampicin (white bars). Bars are means, and lines extending from them are standard deviations. *P* values are given. The adjusted level of significance was $P < .017$ for comparisons with the nonvariant (Student *t* test with Bonferroni adjustment).

in vitro. *SLCO1B1*c.388A>T causes exchange p.Asn130Asp in the second extracellular loop, which affects substrate recognition with different outcome for the transport rate of the respective substrates. The effect of *SLCO1B1*c.521C dominates over *SLCO1B1*c.388T because the *SLCO1B1**15 haplotype, which includes both single nucleotide polymorphisms, has consistently been associated with reduced transport activity (27). For gadoxetic acid, *SLCO1B1*c.388A>T was a gain-of-function variant, whereas *SLCO1B1*c.521T>C (not significant) and the *SLCO1B1**15 haplotype were loss-of-function variants in our stable transfected HEK cells.

*SLCO1B3*c.334G>T is associated with exchange p.Ser112Ala in the third transmembrane helix, which might influence transport characteristics. The variants *SLCO1B3*c.699G>A and *SLCO1B3*c.1564G>T encode amino acid exchanges in the third (p.Met233Ile) and fifth (p.Gly522Cys) extracellular loop, respectively, and therefore may be involved in substrate recognition. The functional consequence of all single

nucleotide polymorphisms, however, is not well understood and contradictory results have been described (25,28,29). In our study, the OATP1B3 protein that contained both p.112Ala and p.233Ile, as well as the p.522Cys variant, showed significantly lower transport activity for BSP and gadoxetic acid. Please note that *SLCO1B3*c.334G>T and *SLCO1B3*c.699G>A are in nearly complete linkage disequilibrium in human subjects, that the variant *SLCO1B3*c.334G/699A (p.112Ala/233Ile) is the most frequent haplotype in white subjects (23), and that the nonvariant *SLCO1B3*c.334T/699G (p.112Ser/233Ile) is a gain-of-function haplotype for the cellular uptake of gadoxetic acid in our in vitro data.

In our clinical study, we confirmed that carriers of at least one *SLCO1B1**5 allele (*SLCO1B1**1a/*5, *SLCO1B1**5/*15, and *SLCO1B1**15/*15) showed significantly reduced liver enhancement at gadoxetic acid-enhanced imaging. This is in line with the overall impression that *SLCO1B1*c.521T>C (p.Val174Ala) is a robust loss-of-function polymorphism for hepatic uptake of gadoxetic acid, as shown before for

many other drugs that were carried in vitro by OATP1B1 p.174Ala, with lower activity compared with the wild-type transport protein (eg, statin drugs, repaglinide, atrasentan, irinotecan, and ezetimibe) (21). In contrast to OATP1B1, the difference in transport activity of OATP1B3 p.112Ala/233Ile versus OATP1B3 p.112Ser/233Ile for gadoxetic acid in vitro did not have any functional correlate in our clinical study; liver enhancement by gadoxetic acid was not significantly different between carriers of the variant haplotype and carriers of the nonvariant haplotype. The functional difference in vitro seems to be too low to influence the overall hepatic uptake rate of gadoxetic acid in vivo.

Identification of OATP1B1 and OATP1B3 as hepatic uptake carriers of gadoxetic acid in human subjects enables prediction of liver enhancement on MR images. Major confounders may be genetic polymorphisms of OATP1B1 and OATP1B3, coadministration of drugs or food ingredients that modulate or regulate the carriers, and liver diseases known to be associated with impaired OATP function.

Figure 3

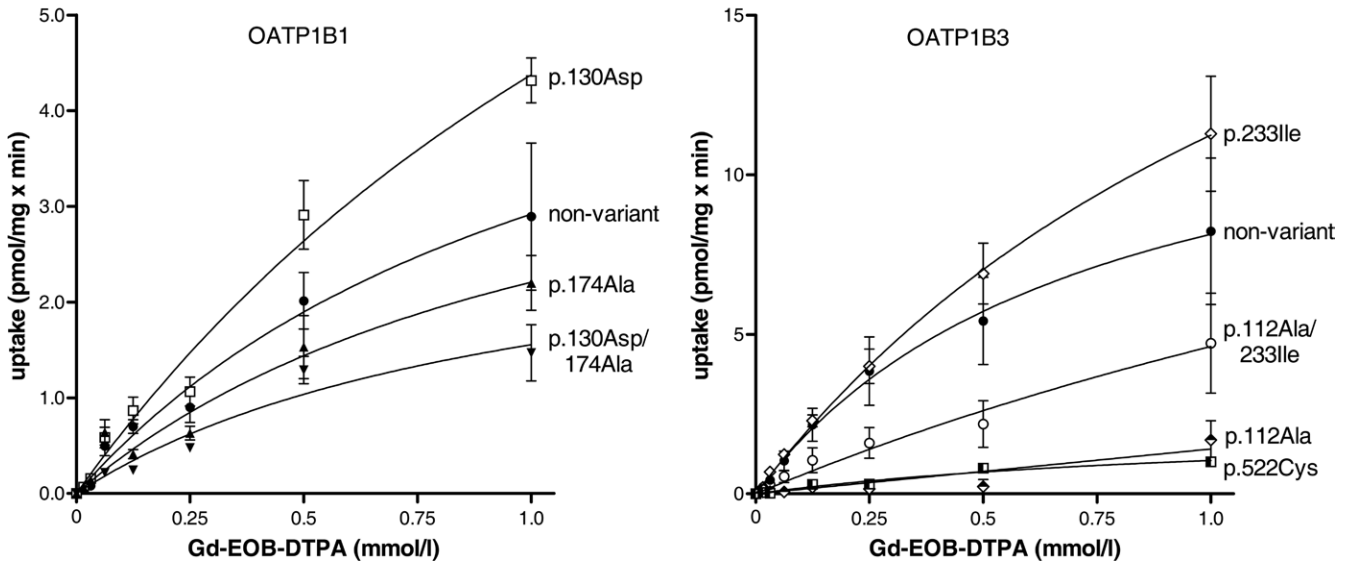


Figure 3: Graphs show uptake of gadoxetic acid in HEK cells expressing nonvariant OATP1B1, OATP1B1 p.130Asp, OATP1B1 p.174Ala, and OATP1B1 p.130Asp/174Ala (left) and nonvariant OATP1B3, OATP1B3 p.112Ala, OATP1B3 p.233Ile, OATP1B3 p.522Cys, and OATP1B3 p.112Ala/233Ile (right). Data points and lines extending from them indicate mean \pm standard deviation.

Table 1

Transport Characteristics for Uptake of Gadoxetic Acid in HEK Cells

Variant	Michaelis-Menten Vonstant (mmol/L)	PValue	Maximum Transport Velocity (pmol/[mg \times min])	PValue
OATP1B1				
Nonvariant	1.17 \pm 0.800	...	6.32 \pm 2.73	...
p.130Asp	1.92 \pm 0.737	.500	12.8 \pm 3.53	.001
p.174Ala	1.15 \pm 0.598	.984	4.75 \pm 1.55	.153
p.130Asp/174Ala	1.00 \pm 0.491	.859	3.11 \pm 0.918	.004
OATP1B3				
Nonvariant	0.532 \pm 0.353	...	7.43 \pm 2.43	...
p.112Ala	0.240 \pm 0.216	.050	0.364 \pm 0.125	.0001
p.233Ile	1.16 \pm 0.674	.025	15.1 \pm 5.52	.002
p.522Cys	0.195 \pm 0.454	.098	0.295 \pm 0.247	.0001
p.112Ala/233Ile	0.964 \pm 0.772	.146	4.46 \pm 2.13	.014

Note.—Unless otherwise indicated, data are mean \pm standard deviation. The adjusted level of significance was $P < .017$ for comparisons with nonvariant OATP1B1 and $P < .013$ for comparisons with nonvariant OATP1B3 (Student *t* test with Bonferroni adjustment).

It should be recognized that hepatic enhancement can be reduced by approximately 30%–40% by genetic polymorphisms of hepatic uptake transporters. In consideration of the fact that the primary use for gadoxetic acid is the depiction of focal liver lesions, the magnitude of this genetic variation could affect the

visualization of lesions in subjects with focal lesions with impaired or lack of positive enhancement (eg, metastases). *SLCO1B1*521T>C, the loss-of-function variant (poor transporter) for gadoxetic acid, has gene frequencies of approximately 15% in white and Asian subjects and approximately 2% in black

subjects (ie, homozygous carriers of that allele are very rare, occurring in no more than 2% of all cases) (21). However, the c.521C allele often occurs in a haplotype with c.388G (*15), the frequency of which is 24% in the United States and 16% in Europe and North Africa (30). Thus, a decreased level of liver enhancement at gadoxetic acid administration frequently may be of genetic origin. Otherwise, polymorphisms of OATP1B3 are most likely not of practical relevance, given that the *SLCO1B3*c.334T/699G haplotype (TT/GG frequency in white subjects is approximately 6%) was not of functional relevance in our clinical study and because *SLCO1B3*c.1564G>T, a major loss-of-function variant in our in vitro study, is rare in white subjects (allelic frequency, 1.9%) (23,28).

To our knowledge, the meaning of drug interactions in the hepatic uptake of gadoxetic acid in human subjects has not been studied thoroughly. However, in rats, the antibiotic rifampicin, which is a strong inhibitor of OATPs, exerted a marked decrease on liver enhancement (17,31). It might be that strong inhibitors of OATP1B1, OATP1B3, or both

Table 2

Pharmacokinetic Characteristics of Gadoxetic Acid in Healthy Subjects Selected According to Functional Relevant Genotypes of *SLC01B1* and *SLC01B3*

Genotype	No. of Subjects	Dose (mg)	AUC ($\mu\text{g} \times \text{h/mL}$)	C_0 ($\mu\text{g/mL}$)	$T_{1/2}$ (h)	CL_R (mL/min)	CL_I (mL/min)	$A_{e, \text{urine}}$ (mg)	$A_{e, \text{feces}}$ (mg)
Wild-type	10	1180 \pm 102	119 \pm 31.7	157 \pm 45.9	15.8 \pm 9.33	74.1 \pm 37.8	87.2 \pm 36.9	500 \pm 219	624 \pm 288
<i>SLC01B1</i>									
*1b/*1b	8	1380 \pm 212	123 \pm 17.0	132 \pm 24.9	13.6 \pm 4.37	87.7 \pm 37.0	87.2 \pm 38.7	634 \pm 210	618 \pm 249
*15/*15	8	1210 \pm 212	120 \pm 31.2	145 \pm 38.2	14.9 \pm 10.5	76.6 \pm 22.5	93.3 \pm 63.3	513 \pm 100	596 \pm 350
*1a/*5	6	1359 \pm 284	133 \pm 31.9	164 \pm 67.3	10.9 \pm 2.92	82.0 \pm 28.8	120 \pm 48.3	627 \pm 244	933 \pm 345
<i>SLC01B3</i> *4/*4	4	1274 \pm 170	105 \pm 12.7	117 \pm 16.6	7.23 \pm 7.54	80.5 \pm 10.2	111 \pm 46.5	501 \pm 52	715 \pm 355

Note.—Data are mean \pm standard deviation. $A_{e, \text{feces}}$ = amount excreted into feces, $A_{e, \text{urine}}$ = amount excreted into urine, AUC = area under the serum concentration-time curve, CL_I = intestinal clearance, CL_R = renal clearance, C_0 = fictive serum concentration at time zero, $T_{1/2}$ = elimination half-life.

Figure 4

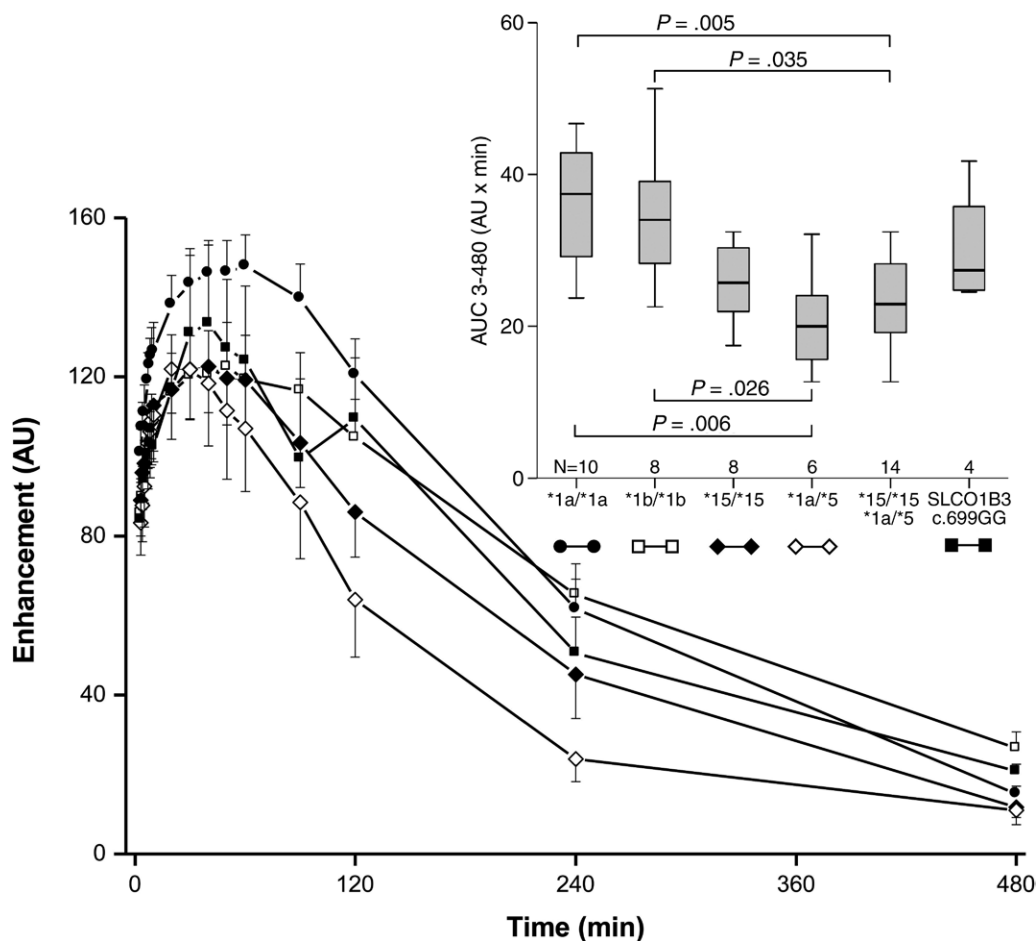


Figure 4: Enhancement time curves (in arbitrary units) and areas under the enhancement curve (inset) of gadoxetic acid in healthy subjects selected according to functional relevant genotypes of *SLC01B1* and *SLC01B3*. On the enhancement time curves, data points and lines extending from them indicate mean \pm standard deviation, respectively, whereas in the box plots, these are indicated by black lines and error bars, respectively. *P* indicates the level of significance (analysis of variance post hoc tests with Bonferroni adjustment).

substantially influence liver enhancement by gadoteric acid in human subjects. Drugs with high inhibitory potency are the cholesterol-lowering agent atorvastatin; immunosuppressants, such as cyclosporine or tacrolimus; the human immunodeficiency virus protease inhibitors nelfinavir, ritonavir, and saquinavir; and glibenclamide, paclitaxel, and rifampicin. It should also be recognized that hyperforin, an ingredient of grapefruit juice, is also a strong OATP1B1 inhibitor, and its potential interaction with gadoteric acid should be evaluated in clinical trials (27). In the meantime, administration of the contrast agent should be avoided if possible, at least during the absorption period (2–3 hours for most of the previously mentioned drugs).

Liver-selective enhancement by gadoteric acid is correlated with the expression of OATP1B1, OATP1B3, or both in hepatocellular carcinoma nodules (10,11). There is ample evidence from liver biopsy studies that expression of the uptake transporters is substantially reduced in patients with cholestatic alcoholic hepatitis (32), primary biliary cirrhosis (33), or hepatitis C virus-related liver cirrhosis (34,35). In patients with chronic liver disease, enhancement by gadoteric acid is closely correlated to the Child-Pugh classification and the disappearance rate of indocyanine green (13,15,36). Because the disappearance rate of indocyanine green is indicated by the expression levels of liver-specific OATP1B1 and OATP1B3 but not by the expression level of the ambiguous OATP2B1 (37), the signal intensity in gadoteric acid-enhanced MR imaging may be a surrogate for the function of hepatic anion uptake transporters in patients with chronic liver disease. However, further clinical research is needed to determine whether quantitative information on liver function (ie, uptake) can be derived from data obtained at liver imaging with gadoteric acid.

The major limitation of our study was the small sample size of subjects with the *SLCO1B3*^{*4/*4} haplotype and the lack of data from

subjects with extremely rare OATP1B3 p.112Ala (*SLCO1B3*c.334G) and OATP1B3 p.522Cys (*SLCO1B3*c.1564T), respectively, which were strong loss-of-function variants for gadoteric acid uptake in vitro. Thus, we could not confirm the functional meaning of OATP1B3 in this pharmacogenetic study in healthy subjects.

In conclusion, the liver-specific human drug transporters OATP1B1 and OATP1B3 are uptake carriers for gadoteric acid, and their activity may be used to predict the signal intensity in gadoteric acid-enhanced liver MR imaging. Genetic polymorphisms of OATP1B1 are a major confounder of reduced signal intensity in healthy subjects.

Acknowledgments: We are grateful to Danilo Wegner, Gitta Schumacher, Sabine Bade, Marten Möller, Andrea Seidel, Gesine Jenz, and Stefan Hadlich for reliable and helpful assistance.

Disclosures of Potential Conflicts of Interest: **A.N.** No potential conflicts of interest to disclose. **J.J.** No potential conflicts of interest to disclose. **M.K.** No potential conflicts of interest to disclose. **S.O.** No potential conflicts of interest to disclose. **C.M.** No potential conflicts of interest to disclose. **S.N.** No potential conflicts of interest to disclose. **W.W.** No potential conflicts of interest to disclose. **N.H.** No potential conflicts of interest to disclose. **W.S.** No potential conflicts of interest to disclose. **J.P.K.** No potential conflicts of interest to disclose.

References

- Clemént O, Mühler A, Vexler VS, et al. Comparison of Gd-EOB-DTPA and Gd-DTPA for contrast-enhanced MR imaging of liver tumors. *J Magn Reson Imaging* 1993;3(1):71–77.
- Hammerstingl R, Huppertz A, Breuer J, et al. Diagnostic efficacy of gadoteric acid (Primovist)-enhanced MRI and spiral CT for a therapeutic strategy: comparison with intraoperative and histopathologic findings in focal liver lesions. *Eur Radiol* 2008;18(3):457–467.
- Vogl TJ, Kümmel S, Hammerstingl R, et al. Liver tumors: comparison of MR imaging with Gd-EOB-DTPA and Gd-DTPA. *Radiology* 1996;200(1):59–67.
- Stern W, Schick F, Kopp AF, et al. Dynamic MR imaging of liver metastases with Gd-EOB-DTPA. *Acta Radiol* 2000;41(3):255–262.
- Tanimoto A, Lee JM, Murakami T, Huppertz A, Kudo M, Grazioli L. Consensus report of the 2nd International Forum for Liver MRI. *Eur Radiol* 2009;19(Suppl 5):S975–S989.
- Zech CJ, Herrmann KA, Reiser MF, Schoenberg SO. MR imaging in patients with suspected liver metastases: value of liver-specific contrast agent Gd-EOB-DTPA. *Magn Reson Med Sci* 2007;6(1):43–52.
- Huppertz A, Haraida S, Kraus A, et al. Enhancement of focal liver lesions at gadoteric acid-enhanced MR imaging: correlation with histopathologic findings and spiral CT—initial observations. *Radiology* 2005;234(2):468–478.
- Saito K, Kotake F, Ito N, et al. Gd-EOB-DTPA enhanced MRI for hepatocellular carcinoma: quantitative evaluation of tumor enhancement in hepatobiliary phase. *Magn Reson Med Sci* 2005;4(1):1–9.
- Kim SH, Kim SH, Lee J, et al. Gadoteric acid-enhanced MRI versus triple-phase MDCT for the preoperative detection of hepatocellular carcinoma. *AJR Am J Roentgenol* 2009;192(6):1675–1681.
- Narita M, Hatano E, Arizono S, et al. Expression of OATP1B3 determines uptake of Gd-EOB-DTPA in hepatocellular carcinoma. *J Gastroenterol* 2009;44(7):793–798.
- Tsuboyama T, Onishi H, Kim T, et al. Hepatocellular carcinoma: hepatocyte-selective enhancement at gadoteric acid-enhanced MR imaging—correlation with expression of sinusoidal and canalicular transporters and bile accumulation. *Radiology* 2010;255(3):824–833.
- Tschirch FT, Struwe A, Petrowsky H, Kalkes I, Marincek B, Weishaupt D. Contrast-enhanced MR cholangiography with Gd-EOB-DTPA in patients with liver cirrhosis: visualization of the biliary ducts in comparison with patients with normal liver parenchyma. *Eur Radiol* 2008;18(8):1577–1586.
- Motosugi U, Ichikawa T, Sou H, et al. Liver parenchymal enhancement of hepatocyte-phase images in Gd-EOB-DTPA-enhanced MR imaging: which biological markers of the liver function affect the enhancement? *J Magn Reson Imaging* 2009;30(5):1042–1046.
- Tajima T, Takao H, Akai H, et al. Relationship between liver function and liver signal intensity in hepatobiliary phase of gadolinium ethoxybenzyl diethylenetriamine pentaacetic acid-enhanced magnetic resonance imaging. *J Comput Assist Tomogr* 2010;34(3):362–366.
- Katsube T, Okada M, Kumano S, et al. Estimation of liver function using T1 mapping on Gd-EOB-DTPA-enhanced magnetic resonance imaging. *Invest Radiol* 2011;46(4):277–283.

16. Clément O, Mühler A, Vexler V, Berthezène Y, Brasch RC. Gadolinium-ethoxybenzyl-DTPA, a new liver-specific magnetic resonance contrast agent. kinetic and enhancement patterns in normal and cholestatic rats. *Invest Radiol* 1992;27(8):612–619.
17. Kato N, Yokawa T, Tamura A, Heshiki A, Ebert W, Weinmann HJ. Gadolinium-ethoxybenzyl-diethylenetriamine-pentaacetic acid interaction with clinical drugs in rats. *Invest Radiol* 2002;37(12):680–684.
18. Schuhmann-Giampieri G, Schmitt-Willich H, Press WR, Negishi C, Weinmann HJ, Speck U. Preclinical evaluation of Gd-EOB-DTPA as a contrast agent in MR imaging of the hepatobiliary system. *Radiology* 1992;183(1):59–64.
19. van Montfoort JE, Stieger B, Meijer DKF, Weinmann HJ, Meier PJ, Fattinger KE. Hepatic uptake of the magnetic resonance imaging contrast agent gadoxetate by the organic anion transporting polypeptide Oatp1. *J Pharmacol Exp Ther* 1999;290(1):153–157.
20. Leonhardt M, Keiser M, Oswald S, et al. Hepatic uptake of the magnetic resonance imaging contrast agent Gd-EOB-DTPA: role of human organic anion transporters. *Drug Metab Dispos* 2010;38(7):1024–1028.
21. International Transporter Consortium, Giacomini KM, Huang SM, et al. Membrane transporters in drug development. *Nat Rev Drug Discov* 2010;9(3):215–236.
22. König J, Seithel A, Gradhand U, Fromm MF. Pharmacogenomics of human OATP transporters. *Naunyn Schmiedebergs Arch Pharmacol* 2006;372(6):432–443.
23. Laitinen A, Niemi M. Frequencies of single-nucleotide polymorphisms of *SLCO1A2*, *SLCO1B3* and *SLCO2B1* genes in a Finnish population. *Basic Clin Pharmacol Toxicol* 2011;108(1):9–13.
24. Seithel A, Eberl S, Singer K, et al. The influence of macrolide antibiotics on the uptake of organic anions and drugs mediated by OATP1B1 and OATP1B3. *Drug Metab Dispos* 2007;35(5):779–786.
25. Franke RM, Baker SD, Mathijssen RH, Schuetz EG, Sparreboom A. Influence of solute carriers on the pharmacokinetics of CYP3A4 probes. *Clin Pharmacol Ther* 2008;84(6):704–709.
26. Oswald S, König J, Lütjohann D, Giessmann T, Kroemer HK, Rimbach C, Roskopf D, Fromm MF, Siegmund W. Disposition of ezetimibe is influenced by polymorphisms of the hepatic uptake carrier OATP1B1. *Pharmacogenet Genomics*. 2008 Jul;18(7):559–68.
27. Kalliokoski A, Niemi M. Impact of OATP transporters on pharmacokinetics. *Br J Pharmacol* 2009;158(3):693–705.
28. Letschert K, Keppler D, König J. Mutations in the *SLCO1B3* gene affecting the substrate specificity of the hepatocellular uptake transporter OATP1B3 (OATP8). *Pharmacogenetics* 2004;14(7):441–452.
29. Schwarz UI, Meyer zu Schwabedissen HE, Tirona RG, et al. Identification of novel functional organic anion-transporting polypeptide 1B3 polymorphisms and assessment of substrate specificity. *Pharmacogenet Genomics* 2011;21(3):103–114.
30. Pasanen MK, Neuvonen PJ, Niemi M. Global analysis of genetic variation in *SLCO1B1*. *Pharmacogenomics* 2008;9(1):19–33.
31. Vavricka SR, Van Montfoort J, Ha HR, Meier PJ, Fattinger K. Interactions of rifamycin SV and rifampicin with organic anion uptake systems of human liver. *Hepatology* 2002;36(1):164–172.
32. Zollner G, Fickert P, Zenz R, et al. Hepatobiliary transporter expression in percutaneous liver biopsies of patients with cholestatic liver diseases. *Hepatology* 2001;33(3):633–646.
33. Zollner G, Fickert P, Silbert D, et al. Adaptive changes in hepatobiliary transporter expression in primary biliary cirrhosis. *J Hepatol* 2003;38(6):717–727.
34. Ogasawara K, Terada T, Katsura T, et al. Hepatitis C virus-related cirrhosis is a major determinant of the expression levels of hepatic drug transporters. *Drug Metab Pharmacokinet* 2010;25(2):190–199.
35. Nakai K, Tanaka H, Hanada K, et al. Decreased expression of cytochromes P450 1A2, 2E1, and 3A4 and drug transporters Na⁺-taurocholate-cotransporting polypeptide, organic cation transporter 1, and organic anion-transporting peptide-C correlates with the progression of liver fibrosis in chronic hepatitis C patients. *Drug Metab Dispos* 2008;36(9):1786–1793.
36. Takao H, Akai H, Tajima T, et al. MR imaging of the biliary tract with Gd-EOB-DTPA: effect of liver function on signal intensity. *Eur J Radiol* 2011;77(2):325–329.
37. Aoki M, Terada T, Ogasawara K, et al. Impact of regulatory polymorphisms in organic anion transporter genes in the human liver. *Pharmacogenet Genomics* 2009;19(8):647–656.